Published in final edited form as:
J Cereb Blood Flow Metab. 2008 May ; 28(5): 995–1008. doi:10.1038/sj.jcbfm.9600597.

Cerebral Blood Flow Heterogeneity in Preterm Sheep: Lack of Physiological Support for Vascular Boundary Zones in Fetal Cerebral White Matter

Melissa McClure[1,5], **Art Riddle**[1,5], **Mario Manese**[1], **Ning Ling Luo**[1], **Dawn A. Rorvik**[4], **Katherine A. Kelly**[4], **Clyde H. Barlow**[4], **Jeffrey J. Kelly**[4], **Kevin Vinecore**[1], **Colin Roberts**[1,2], **A. Roger Hohimer**[3,6], and **Stephen A. Back**[1,2,6,7]

[1] Department of Pediatrics, Oregon Health & Science University, Portland, Oregon and Barlow Scientific Inc

[2] Department of Neurology and Obstetrics, Oregon Health & Science University, Portland, Oregon and Barlow Scientific Inc

[3] Department of Gynecology, Oregon Health & Science University, Portland, Oregon and Barlow Scientific Inc

[4] Department of Chemistry, The Evergreen State College, Olympia Washington

Abstract

Periventricular white matter (PVWM) injury is the leading cause of chronic neurological disability in survivors of prematurity. To address the role of cerebral ischemia in the pathogenesis of this injury, we tested the hypothesis that immaturity of spatially distal vascular “end” or “border” zones predisposes the PVWM to be more susceptible to falls in cerebral blood flow (CBF) than more proximal regions, such as the cerebral cortex. We used fluorescently-labeled microspheres to quantify regional CBF *in situ* in the 0.65 gestation fetal sheep in histopathologically-defined 3-dimensional regions by means of *post hoc* digital dissection and co-registration algorithms.

Basal flow in PVWM was significantly lower than gyral white matter and cerebral cortex, but was equivalent in superficial, middle and deep PVWM. Absolute and relative CBF (expressed as percentage of basal) CBF did not differ during ischemia or reperfusion between the PVWM and more superficial gyral white matter or cortex. Moreover, CBF during ischemia and reperfusion was equivalent at three distinct levels of the PVWM. Absolute and relative CBF during ischemia and reperfusion was not predictive of the severity of PVWM injury, as defined by TUNEL staining. However, the magnitude of ischemia to the cerebral cortex directly correlated with lesion severity ($r = -0.48$, $p < .05$). Hence, the PVWM did not display unique CBF disturbances that accounted for the distribution of injury. These results suggest that previously-defined cellular-maturational factors have a greater influence on the vulnerability of PVWM to ischemic injury than the presence of immature vascular-boundary zones.

INTRODUCTION

Periventricular white matter injury (PWMI) is the major form of brain injury and the leading cause of chronic neurological disability in survivors of premature birth (Volpe, 2000;

[7]Correspondence to: Stephen A. Back, M.D., Ph.D. Department of Pediatrics, Oregon Health & Science University, 3181 SW Sam Jackson Park Road, HRC-5, Portland, Oregon 97239-3098, 503-494-0906 (phone), 503-494-0428 (facsimile), backs@oshus.edu.
[5]These authors contributed equally to this work;
[6]Joint senior authors

Ferriero, 2004). PWMI is observed in up to 25% of preterm survivors who acquire the permanent motor deficits of cerebral palsy and in 25–50% that develop cognitive and learning disabilities by school age (Hack et al., 2005; Miller et al., 2005). Increasing evidence supports that PWMI is initiated in critically ill neonates by cerebral hypoxia-ischemia and accompanying oxidative stress that targets susceptible late oligodendrocyte progenitors (preOLs) (Volpe, 2003; Back, 2006). The spatial distribution of white matter injury is related to the relative density of susceptible preOLs and more resistant myelinating oligodendroyctes (Back et al., 2005; Riddle et al., 2006).

The extent to which spatial heterogeneity of the cerebral vascular supply also contributes to the regional predilection for PWMI remains controversial. It has been proposed that immaturity of micro-vascular end and border zones predisposes the periventricular white matter (PVWM) to hypoperfusion in the setting of systemic hypotension, a common clinical scenario for the critically ill premature neonate (Volpe, 2001). Systemic hypotension may also pose particular risks for the premature infant, because of a lack of cerebral autoregulation (Tsuji et al., 2000; Volpe, 2001; Greisen, 2005). In the setting of a pressure-passive circulation, immature vascular zones may coincide with more severe ischemic injury. However, anatomic support for vascular zones remains inconclusive (Nelson et al., 1991) and virtually no physiologic studies of cerebral blood flow (CBF) have been done. Prior studies have not established a relationship between PWMI and perturbations in periventricular flow. Commonly employed measures of global CBF lack the spatial resolution to define cerebral hemodynamics in human PVWM. In addition, small fetal and neonatal animal models have been uninformative due to a paucity of PVWM, a propensity for mixed gray and white matter injury and the technical limitations of invasive CBF measurements (Back et al., 2006b).

To circumvent these limitations, we developed an *in utero* preparation in the immature instrumented sheep fetus (0.65 gestation). We used fluorescent microspheres to quantify fetal CBF *in situ* in anatomically-defined 3-dimensional regions by means of *post hoc* digital dissection. Global cerebral ischemia-reperfusion was initiated when normal CBF was interrupted by carotid occlusion (Reddy et al., 1998; Riddle et al., 2006). Ischemia, which was severe but not complete, reduced global CBF by approximately 80–90% and generated graded injury to frontal and parietal PVWM, two regions of predilection for human PWMI (Riddle et al., 2006). We tested the hypothesis that spatially distinct vascular “end” or “border” zones exist that predispose more distal regions, such as the PVWM, to be more susceptible to falls in blood flow than more proximal regions, such as the cerebral cortex. To test this hypothesis, we determined if physiologically-distinct zones of CBF were present in PVWM during conditions of basal, ischemia or reperfusion flow. We sought evidence that during global cerebral hypoperfusion, CBF in the deep PVWM fell proportionally more than in more superficial regions of the PVWM, gyral white matter, or cerebral cortex. Lastly, we determined if relatively small prospectively defined focal lesions (identified by TUNEL staining) in either cerebral white or gray matter were associated with more severe ischemia than less damaged regions. We identified distinct regional heterogeneity in basal CBF between cerebral gray and white matter. However, during either ischemia or reperfusion the PVWM was not subject to distinct differences in CBF, nor were more pronounced CBF disturbances identified in regions of the PVWM that were more susceptible to injury.

MATERIALS AND METHODS

Surgical Procedure

An instrumented fetal cerebral hypoperfusion preparation (Reddy et al., 1998) and the general surgical procedures (Chao et al., 1991) were modified as recently described (Riddle et al., 2006). Subjects were time-bred sheep of mixed western breed (91–92 days gestation;

term, 145 days). Fetuses were operated with sterile technique under general anesthesia (1% halothane in O_2 and N_2O). Vinyl catheters were placed in the amniotic cavity and into either a fetal axillary artery or non-occlusively into one carotid artery and a fetal hind-limb vein. Hydraulic occluders (silastic) were placed on each carotid artery. To confine the cerebral blood supply to the carotid arteries, the vertebro-occipital anastomoses were ligated bilaterally. These anastomoses connect the vertebral arteries with the external carotid arteries that are fed by the brachiocephalic artery (Baldwin and Bell, 1963). After closure of the uterus, the lines were externalized and 1 million units of penicillin G were infused into the amniotic cavity. Post-operative housing was on clean dry bedding in an individual cage with access to food and water *ad libitum* as well as with close visual contact with other sheep.

EEG Recording

One or two pairs of EEG electrodes (AS633–5SSF, Cooner Wire, Chatsworth, CA) were secured on the dura over the parasagittal parietal cortex (5 mm and 10 mm anterior to bregma and 5 mm lateral) with a reference electrode attached over the occiput. The electrodes were connected to high impedance amplifiers to provide a filtered input to a Stellate Systems (Montreal, Quebec) digital EEG recording and analysis system. We recorded 2 to 5 channels of continuous EEG from 10 animals for up to 16 hours before and after global ischemia. Seizure detection was done both by visual analysis and confirmed with a newborn seizure detection algorithm from Stellate Systems.

Blood Analysis

One ml blood samples, taken anaerobically from the fetal axillary artery, were analyzed for arterial p_aH, P_aO_2, P_aCO_2 (corrected to 39°C; IL Synthesis 10 pH/Blood Gas Analyzer; Instrumentation Laboratory, Lexington, MA), hemoglobin content (Thb), arterial oxygen content (CaO_2), arterial oxygen saturation ($SatO_2$, IL 682 Co-Oximeter; Instrumentation Laboratory) and hematocrit (Hct, capillary microfuge). Fetuses were only studied if they demonstrated normal fetal oxygenation, defined as >6 ml O_2/100 ml blood, at 24 h recovery from the operation.

Cerebral hypoperfusion studies

Seven animals were studied on the 2nd or 3rd post-operative day. Pressure transducers and a strip-chart recorder (TA 6000; Gould Instruments, Valley View, OH) recorded mean arterial blood pressure (MABP) in the fetal artery relative to amniotic fluid pressure. Fetal heart rate (HR) was calculated from triplicate measurements of the arterial pressure pulse intervals over a continuous recording of >20 seconds. Under basal conditions, physiological parameters and hemodynamic values (HR, MABP, P_aO_2, $SatO_2$ and CaO_2) did not differ significantly between control and experimental groups and were similar to those previously reported (Riddle et al., 2006). Sustained cerebral hypoperfusion of 37 or 45 min duration was initiated by carotid artery occlusion after inflation of the carotid occluders. Cerebral reperfusion was established by deflation of the occluder and was studied at 15 and 60 min following blood flow restoration.

Microsphere injection protocol

Fetal brain blood flow was measured spatially by the fluorescent microsphere distribution and reference sample method (Bernard et al., 2000). Fluorescent microspheres with four different colors (15 μm diameter; F-17047, F-17048, F-17048, F-17050; Molecular Probes, Eugene, OR) had the following peak excitation and emission: green (450/480), yellow (515/534), red (580/605) and scarlet (650/685). Approximately 3×10^6 microspheres suspended in 1 ml of saline with 0.05% Tween were sonicated and then injected over 30

seconds into the fetal hindlimb vein followed by a 2 ml flush with saline. Starting just before and continuing 2 min after each injection, a reference blood sample was drawn at 0.75 ml/min into a syringe mounted in a syringe pump (Harvard Apparatus Co., Dover, MA).

Tissue handling

At 24 hr after the initiation of cerebral reperfusion, the ewe was given an intravenous injection of Euthasol (Virbac Inc, Ft. Worth, TX), to euthanize both ewe and fetus. Fetal brains were collected and immersion fixed at 4°C in 4% paraformaldehyde in 0.1M phosphate buffer, pH 7.4 for 48 hr and then stored in PBS. Brains were subsequently immersed in 20% sucrose until they sank and then were rapidly frozen in OCT.

Acquisition of microsphere distributions with the Imaging CryoMicrotome (ICM)™

Fluorescent microsphere detection and localization was performed with the ICM (Barlow Scientific, Inc., Olympia, WA) (Kelly et al., 2000), which combines fluorescence digital imaging of frozen tissue together with serial cryostat sectioning to determine the three-dimensional (3D) location of each microsphere. The accuracy of the ICM approach for measurement of regional CBF versus radioactive and standard fluorescence microsphere methods has been previously validated (Bernard et al., 2000). The entire frozen fetal brain containing microspheres was mounted in the ICM and serially sectioned to yield ~1000, 38 μm-thick sections. Fluorescence images of the microspheres in the tissue block face were acquired at 25 μm resolution. At regular intervals, adjacent sections were retrieved from the ICM for histological analysis. Fluorescent microspheres in reference blood samples were counted so that the distribution of blood flow could be related to absolute blood flow for each color. A hole drilled into a block of frozen OCT was filled with blood that had been sonicated to disperse microspheres and the sample was frozen rapidly. An aliquot of each reference sample was serially sectioned and imaged as for the tissue samples.

Image Analysis and measurement of Regional Blood Flow

ICM-acquired fluorescence images, were pre-processed to correct for variations in illumination intensity and detector response. The images were analyzed as previously described to distinguish microspheres from background tissue fluorescence and to determine the 3D location of each microsphere (Bernard et al., 2000). Unbiased *in situ* measurements of blood flow were made in frontal and parietal regions in a blinded manner by digital dissection of anatomically defined regions (Gluckman and Parsons, 1983; Vanderwolf and Cooley, 1990). ICM tissue block face images were imported to Amira 3-D image analysis software (TGS, San Diego, CA). All regions were sampled in the coronal plane and contained within a region that extended 4300 μm posterior to the genu of the corpus callosum (frontal blood flow) or posterior to the level of the ventral thalamic nucleus, tail of the caudate and mammillary bodies (parietal blood flow). Analyzed within the frontal region were the cerebral cortex, gyral white matter (GWM), body of the caudate nucleus, head of the caudate nucleus, PVWM, corpus callosum and subventricular zone (SVZ); while the parietal region contained the cortex, GWM, PVWM, hippocampus, and thalamus.

Quantification of terminal deoxynucleotidyltransferase-mediated DUPT (TUNEL) nick end labeled nuclei

We recently showed that counts of TUNEL-labeled nuclei and O4 antibody-labeled degenerating cells were equivalent to quantify cell death in PVWM (Riddle et al., 2006). TUNEL staining was a sensitive and specific marker of total cell degeneration in fetal ovine PVWM. TUNEL-labeled nuclei were visualized in tissue sections obtained from 5 animals and counterstained with methyl green to delineate anatomical boundaries. As shown in figure 1A, digitized images of medial (yellow) and lateral (violet) cortex, medial (blue) and

lateral (brown) GWM and PVWM (green) were acquired (Openlab 4.0.2; Improvision, Boston, MA) using a motorized x-y stage mounted on an inverted microscope (Leica DMIRE2) equipped with a Hammamatsu Orca ER cooled CCD camera. Images were stitched together as a montage with ImageJ software, which resulted in large-scale, high-resolution, 2D images. Each montage comprised a range of 12–60 fields acquired with a 10x objective. Within each montage, ROIs (2.1 ± 0.2 mm^2) were selected of TUNEL-labeled nuclei. These ROIs were confirmed to localize to a minimum of 2 near-adjacent sections (30 μm) from each of two frontal levels separated by ~1500 μm. ROIs were imported into Openlab, and the mean density of TUNEL-labeled nuclei determined using image-threshold analysis software (Improvision; Open Lab) as described (Back et al., 2006a). Within the cerebral white matter (PVWM or GWM), ROIs were defined as $TUNEL_{high}$ (≥10 labeled-nuclei/mm^2) or $TUNEL_{low}$ (<10 labeled-nuclei/mm^2). Cortical ROIs were defined as $TUNEL_{high}$ (≥20 labeled-nuclei/mm^2) or $TUNEL_{low}$ (<20 labeled-nuclei/mm^2).

Co-registration of damage assessment with blood flow (Figure 1)

Individual ROIs of TUNEL-labeled regions were superimposed onto and linked with the low magnification methyl green image (Fig. 1B) and then imported into a commercial 3-D image viewer (Amira). Next, 30–35 fiduciary landmarks (gold spheres in Fig 1B) were matched with the corresponding ICM images (Fig. 1C) for which the unique 3-D location of each green FMS was known. Image 1D was, thus, digitally “warped” to minimize residual spatial error between the landmarks in the blood flow image (Fig. 1C), thereby, precisely co-registering both image data sets. The TUNEL defined ROIs were then identically warped and ROIs of focal damage superimposed onto a 3-D set of ICM images (Fig. 1E). Amira scripts were next executed to count the number of fluorescent microspheres in these damaged and undamaged ROIs in a volume defined by a depth of 1500μm (Fig. 1F). CBF in the ROIs was quantified as ml/min/100g, thus allowing for comparison between CBF and TUNEL density in various regions under basal, occlusion, and reperfusion conditions.

Statistical Analysis

Data Analysis was performed using SPSS 12.0 statistical software. Repeated measures ANOVAs were used for the analysis of differences between independent variables with a time dependent/repeated variable (i.e., blood flow measures taken in the same subjects/groups repeated over time). One-way ANOVAs and independent samples t-tests were done to probe simple effects resulting from repeated measures ANOVAs showing significance, as well as to compare differences between two or more independent variables. One sample t-tests were also done to test differences between single variables expressed as a percentage from a basal score; thus, 100 represents the deviation test value. Lastly, correlations were run, and expressed as Pearson’s r, to determine a within-group linear relationship between two dependent variables.

RESULTS

Basal CBF in the PVWM is significantly lower than in cortical or subcortical gray matter

Frontal and parietal PVWM are two regions of particular predilection for PWMI in human preterm infants. We, thus, first addressed the hypothesis that the susceptibility of the PVWM to ischemia-reperfusion injury is related to vascular boundary zones that manifest as lower basal CBF relative to less vulnerable cortical and subcortical gray matter structures. To test this hypothesis, we quantified basal CBF by *in situ* analysis of fluorescent microsphere distributions in seven anatomically-defined regions at the level of frontal PVWM and four regions at the level of parietal PVWM (Figure 2). Basal CBF in frontal PVWM was very similar to the adjacent corpus callosum and SVZ (Figure 3). Basal CBF was also similar between cortical and subcortical gray matter structures (i.e., cerebral cortex, putamen,

caudate head and caudate body). As a whole, frontal PVWM and adjacent regions (corpus callosum and SVZ) had significantly lower basal CBF compared to cortical and subcortical gray matter structures ($p<0.001$; independent samples t-test). At the parietal level, comparison between cortical and subcortical regions showed that basal CBF in thalamus was significantly higher than the cortex and hippocampus ($p=0.001$; independent samples t-tests). The CBF in the cortex and hippocampus was similar and significantly higher than parietal PVWM ($p<0.001$; independent samples t-test). Thus, CBF was higher in all cortical and subcortical gray matter regions relative to PVWM and adjacent structures during basal conditions, with the thalamus showing the greatest flow.

CBF during ischemia and reperfusion was similar in PVWM and cerebral gray matter structures

We next hypothesized that during global ischemia, the PVWM sustains the most severe reduction in CBF and has the greatest hyperemia during early reperfusion. We first determined that in all regions, CBF during occlusion and reperfusion was independent of the duration of ischemia (37 min, n=3 or 45 min, n=4). A 2 (Occlusion duration; 37 vs. 45 min.) × 3 (CBF event; occlusion, 15 min. reperfusion or 60 min. reperfusion) × 7 (Region) repeated measures ANOVA showed no effect for the duration of ischemia [$F(1,5)= 0.973$] on frontal regional CBFs. A similar analysis of CBF in four parietal regions also showed no effect for the duration of ischemia [$F(1,5)=0.391$]. Hence, in subsequent analyses of both frontal and parietal regions, data was combined for animals subjected to 37 or 45 min of ischemia. There were also no significant differences in CBF between medial and lateral cortex or between medial and lateral GWM (Fig. 1F) and these respective regions were combined for all subsequent analyses.

We next determined mean absolute CBF and mean relative (percentage of basal) CBF values during occlusion and at 15 or 60 min reperfusion for the same seven anatomically-defined frontal and four parietal regions analyzed for basal CBF (Table 1). During ischemia, absolute CBF in all regions was reduced to a similar level. Similarly, there was no significant difference in relative CBF between frontal PVWM, which retained 25% of basal flow during the occlusion and cortical CBF that was reduced to 11% of basal flow. This was the case even though we recently found frontal PVWM to be more susceptible to acute damage than the cerebral cortex (Riddle et al., 2006). Hence, the heterogeneity in CBF under basal conditions was not observed during ischemia.

During early reperfusion (15 min) frontal and parietal cerebral cortex showed a trend towards a modest hypoperfusion state that was not significantly different relative to the corresponding basal CBF. At 60 min reperfusion, there was significant hyperemia in frontal cortex, PVWM and corpus callosum and parietal cortex (one-sample t-tests showing deviation from 100%; $p<0.05$).

Electrographic seizures are delayed beyond the early ischemia-reperfusion period

We hypothesized that electrographic seizures might provide an explanation for the hyperemia that was observed at one hour of reperfusion. Figure 4 (EEG recordings) shows typical electrographic seizures that were seen in all of 10 animals that were recorded for 16 hours after reperfusion. Seizures typically arose from a suppressed background and were brief (<10 sec). Rhythmic slow wave activity (upper panel; 1–1.5 hz) or higher frequency activity (lower panel; 2–3.5 hz) were the predominant patterns seen. Electrographic seizures were rarely seen within the first hour after ischemia (Figure 4, graph). The majority of electrographic seizures were observed between 2 to 6 hours after ischemia, and did not coincide with the first hour of reperfusion when moderate cortical hyperemia was observed.

Gradients of CBF were not present in PVWM

To further test the hypothesis that vascular boundary zones are present in the PVWM, we next determined if gradients of CBF were present between the deep and superficial PVWM. We quantified CBF during basal, ischemia and reperfusion (15 and 60 min) conditions in frontal PVWM that was segmented into six regions (Fig. 5A). The PVWM was divided into medial and lateral regions that were further segmented into inferior, middle and superficial zones. No differences in CBF were found between the medial and lateral frontal PVWM. Accordingly, data for the medial and lateral parts of each zone were grouped in subsequent analyses. Figure 5B shows that no significant differences in CBF were identified among the inferior, middle and superior zones for basal, ischemia, 15 min and 60 min reperfusion conditions. These data, thus, support that no apparent gradients of CBF were present in the frontal PVWM.

PVWM and gyral white matter (GWM) do not differ in absolute or relative CBF

The cerebral white matter of the human premature infant is supplied by short penetrating arteries to the GWM and long penetrating arteries to the PVWM that contribute to apparent vascular end zones (Volpe, 2001). We, thus, next tested the hypothesis that during ischemia the PVWM will sustain more severe ischemia than the GWM. There were significant differences in absolute basal CBF between the PVWM and the GWM for both the frontal (Fig. 6A; $p<0.05$; independent samples t-test) and parietal (Fig. 6B; $p<0.001$) levels. Absolute CBF in frontal (Fig. 6A) and parietal (Fig. 6B) PVWM and GWM showed no significant differences during ischemia or reperfusion (15 min and 60 min). Similarly, there were no significant differences in relative CBF during ischemia or reperfusion between the PVWM and GWM for either the frontal (Fig. 6C) or parietal (Fig. 6D) levels. Hence, there were no differences in absolute or relative CBF between the PVWM or GWM during occlusion or at 15- or 60-min. of reperfusion to support the presence of pathophysiologically significant gradients of flow between superficial and deep cerebral white matter.

CBF during ischemia or reperfusion does not predict the magnitude of histopathologically-defined white matter injury

We next determined if the magnitude and distribution of cerebral white matter injury, defined by TUNEL-staining, coincided with a greater reduction in flow in those regions that sustained greater injury. We hypothesized that regions of more pronounced cerebral white matter injury will show more severe ischemia than regions with minimal injury. To test this hypothesis, we segmented regions of histopathologically-defined injury and co-registered these regions with the corresponding CBF data sets (see Materials and Methods and Figure 1). TUNEL staining was quantified in 17 separate $TUNEL_{high}$ ($\geq$10 labeled-nuclei/mm^2) or 14 $TUNEL_{low}$ (<10 labeled-nuclei/mm^2) lesions in frontal PVWM or GWM. Figure 7A, B shows representative high power images of $TUNEL_{high}$ (A) and $TUNEL_{low}$ (B) ROIs from a portion of a digitized montage in the PVWM. Absolute CBF during ischemia and at 15 min reperfusion showed no significant differences in CBF between $TUNEL_{high}$ and $TUNEL_{low}$ regions in both PVWM (Fig. 7C) and GWM (Fig. 7D) (one-way ANOVA). Similarly, no significant differences were observed for relative CBF in both PVWM (Fig. 7E) and GWM (Fig. 7F). These data support that the distribution of cerebral white matter injury does not appear be related to the magnitude of relative blood flow in cerebral white matter during either ischemia or early-reperfusion.

CBF during ischemia predicts the magnitude of cortical injury

We next determined if the magnitude and distribution of cerebral cortical gray matter injury, defined by TUNEL-staining was related to the degree of CBF reduction during cerebral hypoperfusion. We first segmented medial and lateral regions of frontal cerebral cortex (Fig.

1F). At both levels, medial and lateral regions of cerebral cortex did not differ in CBF for either basal, ischemia or early reperfusion (15 min) CBF. In subsequent studies, medial and lateral regions of cerebral cortex were jointly analyzed. TUNEL staining was quantified in 10 separate $TUNEL_{high}$ (≥20 labeled-nuclei/mm^2) or 8 $TUNEL_{low}$ (<20 labeled-nuclei/mm^2) lesions in frontal cortical gray matter (see Materials and Methods). Figure 8A, B shows representative high power images of $TUNEL_{high}$ (A) and $TUNEL_{low}$ (B) ROIs from a portion of a digitized montage of two adjacent frontal cortical gyri. Cerebral cortical lesions that were $TUNEL_{high}$ showed a significantly greater reduction in absolute CBF during ischemia than regions that were $TUNEL_{low}$ (Fig. 8C; one way ANOVA; [$F(1,16)=10.3$, $p=0.005$]). Analysis of relative CBF in $TUNEL_{high}$ and $TUNEL_{low}$ regions showed a similar but not significant trend (Fig. 8D; $p=0.12$). Consistent with these findings, we found that during ischemia there was a significant negative correlation between the magnitude of absolute CBF and the density of TUNEL-labeled cells in a given lesion ($r=-0.48$, $p=0.044$). Hence, the predilection for cortical injury was associated with the severity of ischemia.

DISCUSSION

In order to address the role of physiologically-defined vascular boundary-zones in immature cerebral white matter injury, we developed a novel method to spatially quantify fetal CBF in histopathologically-defined lesions in two regions of predilection for injury in the preterm infant. This study yielded the following findings that failed to support the presence of pathologically significant gradients of fetal CBF under conditions of ischemia or reperfusion: (1) CBF during ischemia and reperfusion was equivalent throughout the PVWM. (2) Absolute and relative CBF did not differ significantly during ischemia or reperfusion between the PVWM and more superficial gyral white matter. (3) Relative CBF in cerebral cortex during ischemia was lower than in PVWM. (4) Relative CBF during ischemia and reperfusion was not predictive of the severity of white matter injury. (5) The magnitude of ischemia to the cerebral cortex but not to the PVWM directly correlated with lesion severity defined by TUNEL staining. Hence, relative to other regions of cerebral white matter, the PVWM did not display unique CBF disturbances. PVWM lesions did not localize to regions susceptible to greater hypoperfusion; nor did less vulnerable regions of the PVWM have greater CBF during ischemia.

In order to test the hypothesis that PVWM injury is related to regional heterogeneities of CBF, the present study took several departures from prior studies that quantified regional fetal CBF with radioactively-labeled microspheres. Because of several limitations of radioactive microspheres, earlier studies provided limited information about regional differences in preterm CBF. Precise definition of regional boundaries in fresh unfixed tissue is not possible. There is, thus, the potential for systematic error in the selection of tissue samples at necropsy. Histological studies are also not feasible in tissue from which radioactive microspheres are extracted. These limitations were circumvented by using fluorescently-labeled microspheres (Riddle et al., 2006). Our approach allowed CBF to be quantified in an unbiased fashion by co-registration of microsphere data sets with histologically-defined regions of interest. A particular advantage of this approach, especially for large animal studies, is that a single microsphere data set can be analyzed in conjunction with multiple histopathological data sets.

Despite these inherent differences in approach, our fetal CBF measurements were in general agreement with previous studies of global CBF with radioactive microspheres (Szymonowicz et al., 1988; Gleason et al., 1989; Iwamoto et al., 1989; Szymonowicz et al., 1990; Helou et al., 1994). We found that basal blood flow in both frontal and parietal PVWM was ~60–70% lower than in the overlying cerebral cortex. Similarly, a prior study of undefined cerebral white matter found ~50% lower rates of basal perfusion than in cortex in

preterm and near term sheep (Szymonowicz et al., 1988). As an isolated finding, the low basal flow in PVWM relative to gray matter does not appear to support the notion of vascular immaturity or insufficiency. Regional differences in basal CBF are more likely related to differences in metabolic demand and a tight linkage between metabolism and blood flow. Basal glucose metabolism in ~0.65 gestation ovine PVWM is about 70% lower than in cerebral cortex (Abrams et al., 1984; Iwamoto et al., 1989). Regional differences in basal flow and metabolism may also be related to the different cell types present in white matter/SVZ versus gray matter or to different levels of neuronal activity.

Despite significant differences in basal CBF in deeply-situated cerebral structures relative to more superficial structures, these differences were not accompanied by pathophysiologically significant differences in CBF during ischemia. In fact, during ischemia absolute and relative CBF were similar. Similarly, in response to hemorrhagic hypotension, both cerebral cortical and white matter blood flow decreased proportionally by about 25% from control levels and did not recover even after re-infusion of blood (Szymonowicz et al., 1990).

The significance of the approximately 30% hyperemia we found in most brain regions at 1-hour of reperfusion remains to be determined. This increased flow does not appear to be associated with seizure activity that was maximal several hours later. We are aware of only one other study that measured reperfusion blood flow in the immature sheep fetus. Re-infusion of blood after hemorrhagic hypotension resulted in a similar modest sustained hypoperfusion in white and gray matter (Szymonowicz et al., 1990). Late gestation fetuses had a substantial hyperemia to many brain regions that was not statistically significant before 12 hours after ischemia (Raad et al., 1999). Post-ischemia hyperemia has been linked to cerebral edema (Heiss et al., 1976).

An advantage of our approach relative to prior studies is that serial measurements of basal, ischemia and early reperfusion flow were feasible in the same animal. We chose to measure CBF at the 15- and 60-minute reperfusion times, because we expected that white matter injury may be related to a rise in free radical generation during the immediate reperfusion period. In adult rodents, major disturbances in reperfusion flow, either high or low, have be associated with increased tissue oxidative damage (Pulsinelli et al., 1982; Katz et al., 1998). However, in agreement with a recent study in preterm sheep (Welin et al., 2005), we did not detect a significant increase in F_2-isoprostanes in tissue collected from the PVWM in three animals at 30 min of reperfusion after 45 min of ischemia (Back, Hohimer and Montine, unpublished findings).

It has been suggested that the predilection for PVWM injury during ischemia is related to a loss of cerebral autoregulation (pressure passive flow) while other regions like the cortex are relatively protected because they can autoregulate (Volpe, 2003; Greisen, 2005). Immature fetal sheep do not appear to autoregulate flow in the cortex, white matter, thalamus or brainstem (Szymonowicz et al., 1990; Muller et al., 2002) and data are also controversial in human (Menke et al., 1997; Tyszczuk et al., 1998; Tsuji et al., 2000; Greisen, 2005). While our experiments were not designed to directly address this hypothesis, our current data do not support that explanation. Absolute and relative CBF were similar between cerebral cortex and PVWM during ischemia. If anything, the PVWM seemed to retain a greater percentage of basal flow than the cortex. Thus, both relatively protected and vulnerable regions with reference to damage have indistinguishable flow characteristics in this particular model of global cephalic hypotension.

Our physiological findings are not consistent with the notion of distinct vascular-anatomic boundary zones in the PVWM as the basis for the predilection to ischemic injury. In human preterm infants, it has been proposed that the distribution of PVWM lesions is explained by

two distinct types of vascular supply that form micro-vascular boundary zones. The first are so-called “ventriculopetal” capillary beds that course from the cortical surface toward the lateral ventricles. Ventriculopetal arteries arise from leptomeningeal arteries, penetrate the cerebral cortex and terminate as capillary endzones adjacent to the ventricles (Lewis, 1957; Strong, 1964). The second are so-called “ventriculofugal arteries that arise from choroidal and striate arteries, project toward the lateral ventricles and then deviate away from the ventricle toward their final termination in a vascular capillary bed in the PVWM (van den Bergh and van der Eecken, 1968; van den Bergh, 1969; Nakamura et al., 1994). In addition to the ventriculopetal endzones, it was proposed that the ventriculopetal and ventriculofugal arteries also collectively give rise to a vascular border zone in the PVWM. The existence of this vascular border zone and the associated ventriculofugal arteries has been the subject of considerable controversy (Mayer and Kier, 1991; Nelson et al., 1991; Volpe, 2001). We previously found that relatively large adjacent regions of medial or lateral PVWM did not differ in CBF under conditions of basal or ischemia-reperfusion flows (Riddle et al., 2006). Here we found that microvascular heterogeneities in flow also did not correlate in magnitude with the severity of PVWM injury.

An alternative explanation for the topography of PVWM lesions is the distribution of susceptible cell types. We recently studied the relative susceptibility of axons and several glia cell types (i.e., microglia-macrophages, astroctytes and oligodendrocyte-lineage cells) to global ischemia in the 0.65 gestation sheep (Riddle et al., 2006). The distribution of ischemic PVWM injury coincided with the magnitude and distribution of degeneration of preOLs. PreOLs are particularly susceptible to oxidative stress and hypoxia-ischemia in human preterm white matter and in fetal sheep (Haynes et al., 2003; Back et al., 2005; Riddle et al., 2006). By contrast, other cell types in the PVWM are markedly more resistant to degeneration triggered by ischemia. In fact, more differentiated OLs were also more resistant to degeneration than preOLs (Riddle et al., 2006). This resistance of OLs to ischemia coincides with an overall lower amount of pathology in OL-rich regions of PVWM. Injury to the PVWM and the gryal WM was, thus, variable, and greatest in preOL-enriched regions. Our present findings suggest that the discrete differences in PVWM injury observed here are related to heterogeneities in the distributions of susceptible cell types.

The susceptibility of cerebral gray matter to ischemia appears to be defined by vascular mechanisms distinct from those that injure white matter. In contrast to the PVWM, the severity of cortical gray matter injury was predicted by the reduction in CBF during ischemia. We recently reported that cortical injury was also proportional to the duration of ischemia between 30 and 45 minutes, and beyond 37 minutes increased markedly both in magnitude and distribution in a nonlinear fashion (Riddle et al., 2006). With prolonged ischemia (45 min), pronounced cortical injury predominated in the medial cortex in a watershed pattern. Our findings suggest the possibility that the vasculature of the cortical gray matter contains physiologically distinct micro-vascular zones. Such zones might arise from heterogeneity in the anatomical maturation of the cortical vasculature. There may also be maturation-dependent heterogeneity in the expression of substances that regulate cerebral vasodilation. Regional differences may also exist in the closing pressure at which CBF approaches a no-flow state (Greisen 2005).

Clinico-pathological Significance

Although a growing body of evidence supports a role for cerebral ischemia in the pathogenesis of white matter injury in critically ill premature infants, routine clinical monitoring of CBF to identify high-risk infants has not yet proven feasible. One potential approach for bed-side clinical monitoring of global CBF is near infared spectroscopy (NIRS), which may provide an indirect measure of PVWM flow. A limitation of NIRS is that CBF measurements are restricted to superficial cerebral cortex (Wolfberg and du

Plessis, 2006). It is also unknown if cortical CBF measurements accurately reflect changes in CBF deeper in the PVWM. The fact that heterogeneity in PVWM injury did not coincide with the magnitude of CBF disturbances further suggests that NIRS may provide a useful indirect means to identify those critically-ill neonates at risk for hypoperfusion of the PVWM. The heterogeneity in cortical CBF that we identified during ischemia also indicates that clinical measurements may require greater sensitivity to discriminate maturation-dependent differences in micro-regional cortical CBF.

In summary, our studies to date support that ischemia-reperfusion injury is a clinically important cause of PVWM injury in human preterm neonates via mechanisms that involve significant oxidative stress. Our studies in preterm fetal sheep suggest that human cerebral white matter lacks physiologically significant vascular boundary zones as the basis for the topography of white matter pathology. Rather, the topography appears to be better explained by the distribution of susceptible preOLs in regions subject to relatively uniform disturbances in CBF during ischemia-reperfusion. Future clinical studies are needed in preterm neonates that apply emerging real-time perfusion imaging approaches to define the degree of CBF heterogeneity under basal conditions and conditions of metabolic demand.

Acknowledgments

This work was supported by grants to SAB from the National Institute of Health (NIH) (KO2 NS41343 and RO1 NS045737), from the Medical Research Foundation of Oregon and the Dickinson Foundation. We are grateful for the support of Dr. Lowell Davis, Dr. John Bissonnette, Dr. Kent Thornburg and the Oregon Heart Center and the technical support of Loni Socha, Robert Webber and Dr. Samantha Lovey.

References

Abrams RM, Ito M, Frisinger JE, Patlak CS, Pettigrew KD, Kennedy C. Local cerebral glucose utilization in fetal and neonatal sheep. Am J Physiol. 1984; 246:R608–618. [PubMed: 6720932]

Back S, Craig A, Luo N, Ren J, Akundi R, Rebeiro I, Rivkees S. Protective effects of caffeine on chronic hypoxia-induced perinatal white matter injury. Ann Neurol. 2006a; 60:696–705. [PubMed: 17044013]

Back SA. Perinatal white matter injury: The changing spectrum of pathology and emerging insights into pathogenetic mechanisms. MRDD Res Rev. 2006; 12:129–140.

Back SA, Riddle A, Hohimer AR. Role of instrumented fetal sheep preparations in defining the pathogenesis of human periventricular white matter injury. Journal of Child Neurology. 2006b; 21:582–589. [PubMed: 16970848]

Back SA, Luo NL, Mallinson RA, O'Malley JP, Wallen LD, Frei B, Morrow JD, Petito CK, Roberts J, CT, Murdoch GH, Montine TJ. Selective vulnerability of preterm white matter to oxidative damage defined by F_2-isoprostanes. Ann Neurol. 2005; 58:108–120. [PubMed: 15984031]

Baldwin B, Bell F. The anatomy of the cerebral circulation of the sheep and ox. The dynamic distribution of the blood supplied by the carotid and vertebral arteries to cranial regions. J Anat, Lond. 1963; 97:203–215. [PubMed: 13969329]

Bernard SL, Ewen JR, Barlow CH, Kelly JJ, McKinney S, Frazer DA, Glenny RW. High spatial resolution measurements of organ blood flow in small laboratory animals. Am J Physiol Heart Circ Physiol. 2000; 279:H2043–H2052. [PubMed: 11045936]

Chao CR, Hohimer AR, Bissonnette JM. Fetal cerebral blood flow and metabolism during oligemia and early postoligemic reperfusion. J Cereb Blood Flow Metab. 1991; 11:416–423. [PubMed: 2016348]

Ferriero DM. Neontal brain injury. New England Journal of Medicine. 2004; 351:1985–1995. [PubMed: 15525724]

Gleason CA, Hamm C, Jones MD Jr. Cerebral blood flow, oxygenation, and carbohydrate metabolism in immature fetal sheep in utero. Am J Physiol. 1989; 256:R1264–R1268. [PubMed: 2735451]

Gluckman P, Parsons Y. Stereotaxic method and atlas for the ovine fetal forebrain. J Dev Physiol. 1983; 5:101–128. [PubMed: 6343472]

Greisen G. Autoregulation of cerebral blood flow in newborn babies. Early Human Develoment. 2005; 81:423–428.

Hack M, Taylor H, Drotar D, Schluchter M, Cartar L, Andreias L, Wilson-Costello D, Klein N. Chronic conditions, functional limitations, and special health care needs of school-aged children born with extremely low-birth-weight in the 1990's. JAMA. 2005; 294:318–325. [PubMed: 16030276]

Haynes RL, Folkerth RD, Keefe RJ, Sung I, Swzeda LI, Rosenberg PA, Volpe JJ, Kinney HC. Nitrosative and oxidative injury to premyelinating oligodendrocytes in periventricular leukomalacia. J Neuropathol Exp Neurol. 2003; 62:441–450. [PubMed: 12769184]

Heiss WD, Hayakawa T, Waltz AG. Cortical neuronal function during ischemia. Effects of occlusion of one middle cerebral artery on single-unit activity in cats. Arch Neurol. 1976; 33:813–820. [PubMed: 999544]

Helou S, Koehler RC, Gleason CA, Jones MD, Traystman RJ. Cerebrovascular Autoregulation During Fetal Development in Sheep. Am J Physiol. 1994; 266:H1069–H1074. [PubMed: 8160810]

Iwamoto HS, Kaufman T, Keil LC, Rudolph AM. Responses to acute hypoxemia in fetal sheep at 0.6–0.7 gestation. Am J Physiol. 1989; 256:H613–620. [PubMed: 2923229]

Katz LM, Callaway CW, Kagan VE, Kochanek PM. Electron spin resonance measure of brain antioxidant activity during ischemia/reperfusion. Neuroreport. 1998; 9:1587–1593. [PubMed: 9631471]

Kelly J, Ewen J, Bernard S, Glenny R, Barlow C. Regional blood flow measurements from fluorescent microsphere images using an imaging cryomicrotome. Rev Sci Instr. 2000; 71:228–234.

Lewis O. The form and development of blood vessels of the mammalian cerebral cortex. J Anat. 1957; 91:40–48. [PubMed: 13405812]

Mayer PL, Kier EL. The controversy of the periventricular white matter circulation: a review of the anatomic literature. 1991; 12:223–228.

Menke J, Michel E, Hildebrand S. Cross-spectral analysis of cerebral autoregulation dynamics in high risk preterm infants during the perinatal period. Pediatr Res. 1997; 42:690–699. [PubMed: 9357945]

Miller SP, Ferriero DM, Leonard C, Piecuch R, Glidden D, Partridge JC, Perez M, Mukherjee P, Vigneron D, Barkovich AJ. Early brain injury in premature newborns detected with magnetic resonance imaging is associated with adverse neurodevelopmental outcome. J Pediatr. 2005; 147:609–616. [PubMed: 16291350]

Muller T, Lohle M, Schubert H, Bauer R, Wicher C, Antonow-Schlorke I, Sliwka U, Nathanielsz P, Schwab M. Developmental changes in cerebral autoregulatory capacity in the fetal sheep parietal cortex. J Physiol. 2002; 539:957–967. [PubMed: 11897864]

Nakamura Y, Okudera T, Hashimoto T. Vascular architecture in white matter of neonates: its relationship to periventricular leukomalacia. J Neuropath Exp Neurol. 1994; 53:582–589. [PubMed: 7964899]

Nelson MD Jr, Gonzalez-Gomez I, Gilles FH. Dyke Award. The search for human telencephalic ventriculofugal arteries. 1991; 12:215–222.

Pulsinelli WA, Levy DE, Duffy TE. Regional cerebral blood flow and glucose metabolism following transient forebrain ischemia. Ann Neurol. 1982; 11:499–502. [PubMed: 7103426]

Raad RA, Tan WK, Bennet L, Gunn AJ, Davis SL, Gluckman PD, Johnston BM, Williams CE. Role of the cerebrovascular and metabolic responses in the delayed phases of injury after transient cerebral ischemia in fetal sheep. Stroke. 1999; 30:2735–2741. [PubMed: 10583005]

Reddy K, Mallard C, Guan J, Marks K, Bennet L, Gunning M, Gunn A, Gluckman P, Williams C. Maturational change in the cortical response to hypoperfusion injury in the fetal sheep. Pediatr Res. 1998; 43:674–682. [PubMed: 9585015]

Riddle A, Luo N, Manese M, Beardsley D, Green L, Rorvik D, Kelly K, Barlow C, Kelly J, Hohimer A, Back S. Spatial heterogeneity in oligodendrocyte lineage maturation and not cerebral blood flow predicts fetal ovine periventricular white matter injury. Journal of Neuroscience. 2006; 26:3045–3055. [PubMed: 16540583]

Strong L. The early embryonic pattern of internal vascularization of the mammalian cerebral cortex. J Comp Neurol. 1964; 123:121–138. [PubMed: 14199263]

Szymonowicz W, Walker AM, Cussen L, Cannata J, Yu VY. Developmental changes in regional cerebral blood flow in fetal and newborn lambs. Am J Physiol. 1988; 254:H52–H58. [PubMed: 3337259]

Szymonowicz W, Walker A, Yu V, Stewart M, Cannata J, Cussen L. Regional cerebral blood flow after hemorrhagic hypotension in the preterm, near-term, and newborn lamb. Pediatr Res. 1990; 28:361–366. [PubMed: 2235134]

Tsuji M, Saul J, du Plessis A, Eichenwald E, Sobh J, Crocker R, Volpe J. Cerebral intravascular oxygenation correlates with mean arterial pressure in critically ill premature infants. Pediatrics. 2000; 106:625–632. [PubMed: 11015501]

Tyszczuk L, Meek J, Elwell C, JSW. Cerebral blood flow is independent of mean arterial blood pressure in preterm infants undergoing intensive care. Pediatrics. 1998; 102:337–341. 400w. [PubMed: 9685435]

van den Bergh R. Centrifigal elements in the vascular pattern of the deep intracerebral blood supply. Angiology. 1969; 20:88–94. [PubMed: 4179336]

van den Bergh R, van der Eecken H. Anatomy and embryology of cerebral circulation. Prog Brain Res. 1968; 30:1–25.

Vanderwolf, C.; Cooley, R. The sheep brain: a photographic series. 2. London, Ontario, Canada: A. J. Kirby Co; 1990.

Volpe JJ. Neurobiology of periventricular leukomalacia in the premature infant. Pediatr Res. 2001; 50:553–562. [PubMed: 11641446]

Volpe JJ. Cerebral white matter injury of the premature infant-more common than you think. Pediatrics. 2003; 112:176–180. [PubMed: 12837883]

Welin A-K, Sandberg M, Lindblom A, Arvidsson P, Nilsson U, Kjellmer I, Mallard C. White matter injury following prolonged free radical formation in the 0.65 gestation fetal sheep brain. Pediatr Res. 2005; 58:100–105. [PubMed: 15879295]

Wolfberg A, du Plessis A. Near-infrared spectroscopy in the fetus and neonate. Clin Perinatol. 2006; 33:707–728. [PubMed: 16950321]

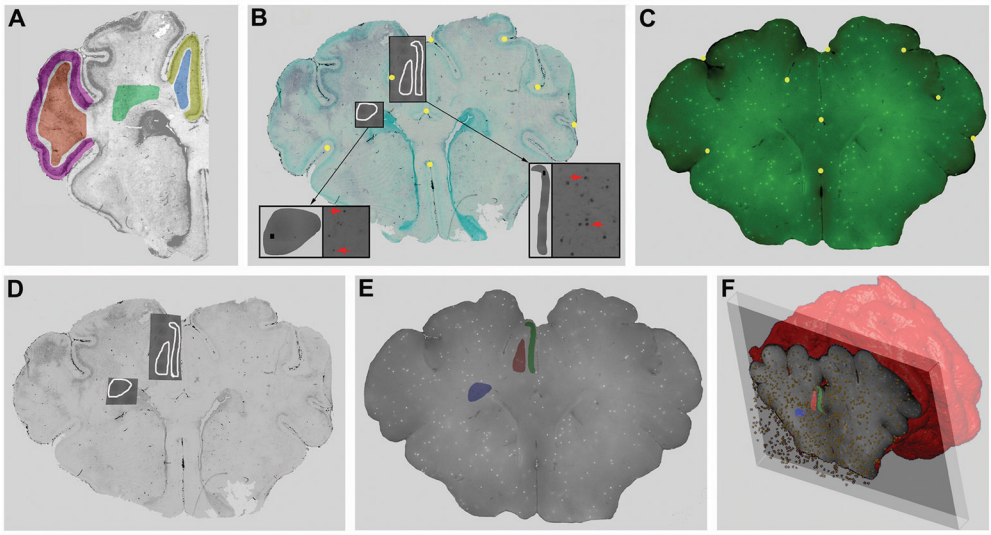

Figure 1.

Our approach for 3-D co-registration and analysis of CBF and cerebral injury data sets acquired from the same brain. A, Representative regions of the medial (yellow) and lateral (violet) cortex, lateral (brown) and medial (blue) gyral white matter and PVWM (green). Low-power montages of digitized images of TUNEL-labeling were generated for each entire region. From within these regions, TUNEL-labeled ROIs were selected. B, A typical tissue section stained for TUNEL and counterstained with methyl green to define anatomical boundaries. For example, 3 TUNEL-labeled ROIs (white tracings) were analyzed in parasagittal cortex, adjacent gyral white matter and PVWM. The higher magnification pull-out panels (arrows) show digitized 10x images of TUNEL+ cells (left, red). These images were stitched together with ImageJ software to generate a montage of the ROIs (gray ROI overlays; right) from which the mean density of TUNEL-labeled cells was determined. Individual ROIs were superimposed onto and linked with the low magnification methyl green image and then imported into a commercial 3-D image viewer (Amira). 30–35 fiduciary landmarks (gold circles) in “B” were matched with the corresponding ICM image (C) for which the unique 3-D location of each green fluorescent microsphere was known. The resulting low-power image in “D” was, thus, digitally “warped” to minimize residual spatial error between the landmarks in “B” and “C”; thereby, precisely co-registering both image data sets. E, The TUNEL-defined ROIs were identically warped onto image “D.” Next, these ROIs of focal damage were superimposed onto a 3-D set of ICM images to generate “E”. F, Amira scripts were next executed to count the number of fluorescent microspheres in the TUNEL-defined ROIs with a depth of 1500μm (E).

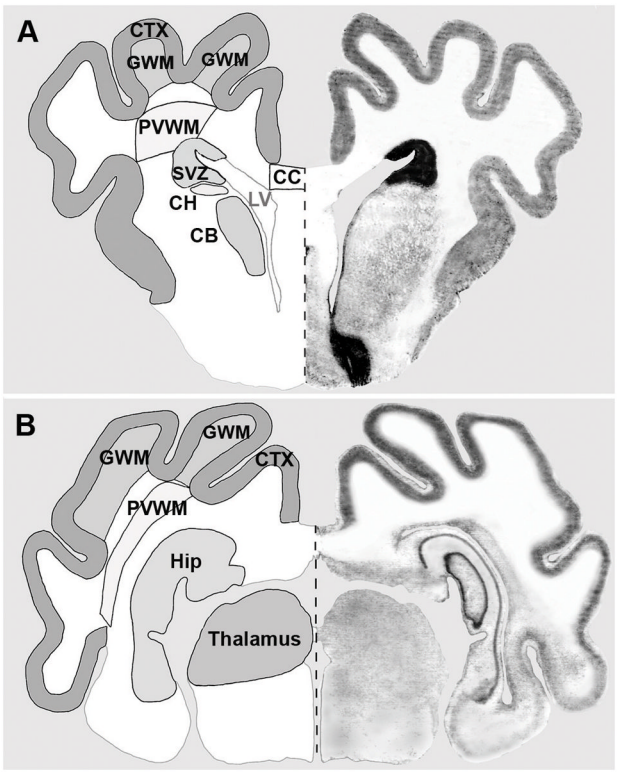

Figure 2.
To determine distinct regional CBF values prior to, during, and at 15 and 60 min after ischemia (see Table 1), the brain was segmented into distinct frontal (A) regions and parietal (B) ROIs. A, Representative frontal ROIs were: cerebral cortex (CTX), gyral white matter (GWM), periventricular white matter (PVWM), subventricular zone (SVZ), corpus callosum (CC), head of the caudate nucleus (CH), and body of the caudate nucleus (CB). B, Representative parietal ROIs were: CTX, GWM, PVWM, hippocampus (Hip), and thalamus.

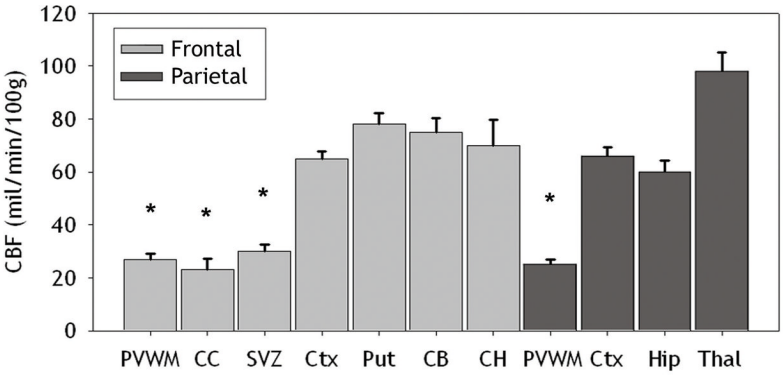

Figure 3.

Basal CBF values (mean±SEM) are shown for seven frontal and four parietal regions. These areas included the periventricular white matter (PVWM), corpus callosum (CC), subventricular zone (SVZ), cortex (Ctx), putamen (Put), caudate body (CB), caudate head (CH), hippocampus (Hip), and thalamus (Thal). There were significant differences (*$p<.001$) between deep cerebral structures (PVWM, SVZ and CC) and all gray matter structures.

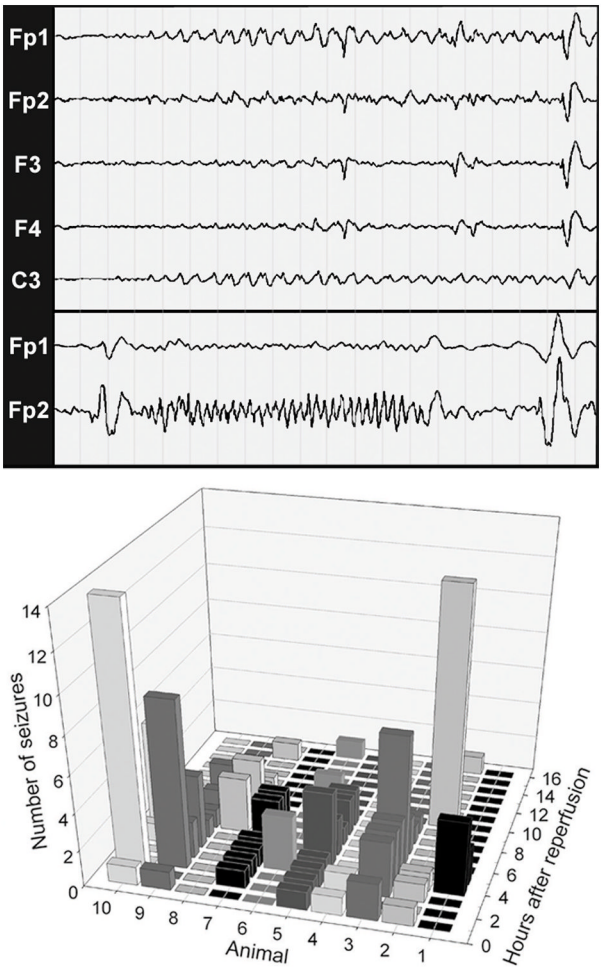

Figure 4.

Electrographic seizures are delayed beyond the early ischemia-reperfusion period. EEG tracings from recordings done during reperfusion. Representative electrographic seizures from different animals are shown in the upper and lower panels. The upper panel shows the initiation of a rhythmic slow wave (1–1.5 hz) seizure of left hemispheric origin that arises from a suppressed background. These slow wave patterns are typical for seizures seen in human neonates (25–44 weeks gestation). Interestingly, they evolve in frequency and amplitude but remain focal, which may relate to the lack of mature myelination at 0.65 gestation. In the lower panel, a faster (2–3.5 hz) seizure is shown that lasts for 12 sec. Higher frequency patterns co-exist with slow wave seizures in preterm neonates. As shown graphically, electrographic seizures, recorded for a 16 h duration in 10 animals, were rare in the first hour after reperfusion. Between 2–6 h there was a marked increase in seizure frequency in the majority of animals and then a diminishing number of events were seen in the last 10 hours. Scale for EEG recordings: 1 page = 20 sec.

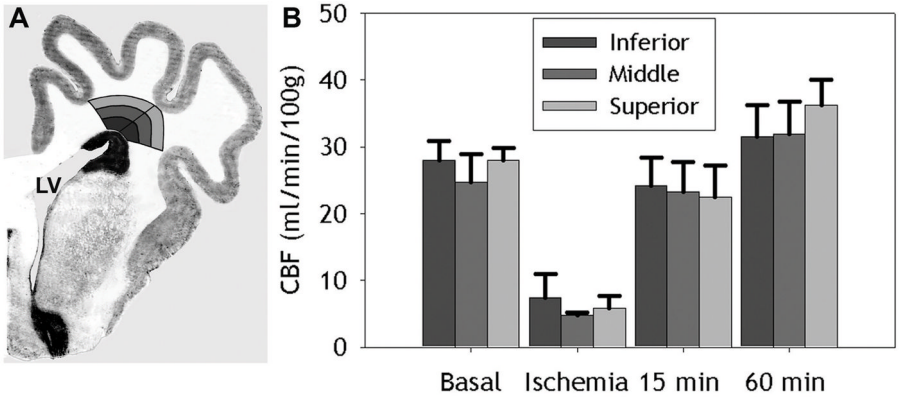

Figure 5.

A, Representative segmentation of the PVWM into medial and lateral sections, both of which were further segmented into inferior, middle, and superior regions of the PVWM. No differences were found between basal CBF values in medial and lateral PVWM. B, Basal CBF values (mean ± SEM) for the entire inferior, middle and superior PVWM. No differences were seen between these segmented regions of the PVWM.

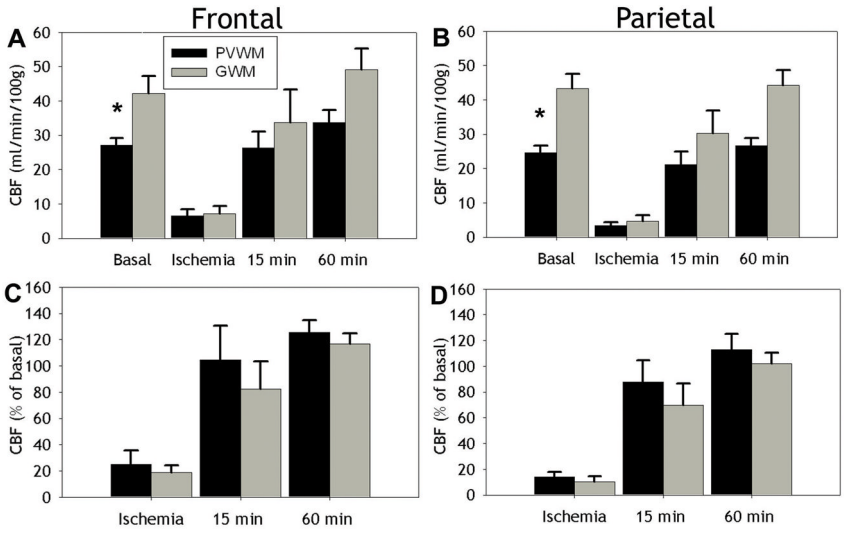

Figure 6.

A, B, Absolute CBF values (mean ± SEM) in PVWM (black bars) and GWM (gray bars) at frontal (A) and parietal (B) levels during basal, ischemia and reperfusion conditions (15 min and 60 min). Basal CBF was significantly lower in PVWM relative to GWM (*p<0.05). No differences were seen, however, between absolute CBF during ischemia or reperfusion. C, D, No differences were seen in relative CBF values, expressed as a percentage of basal flow (mean ± SEM), obtained for PVWM and GWM at frontal (C) and parietal (D) levels during ischemia and reperfusion conditions (15 min and 60 min).

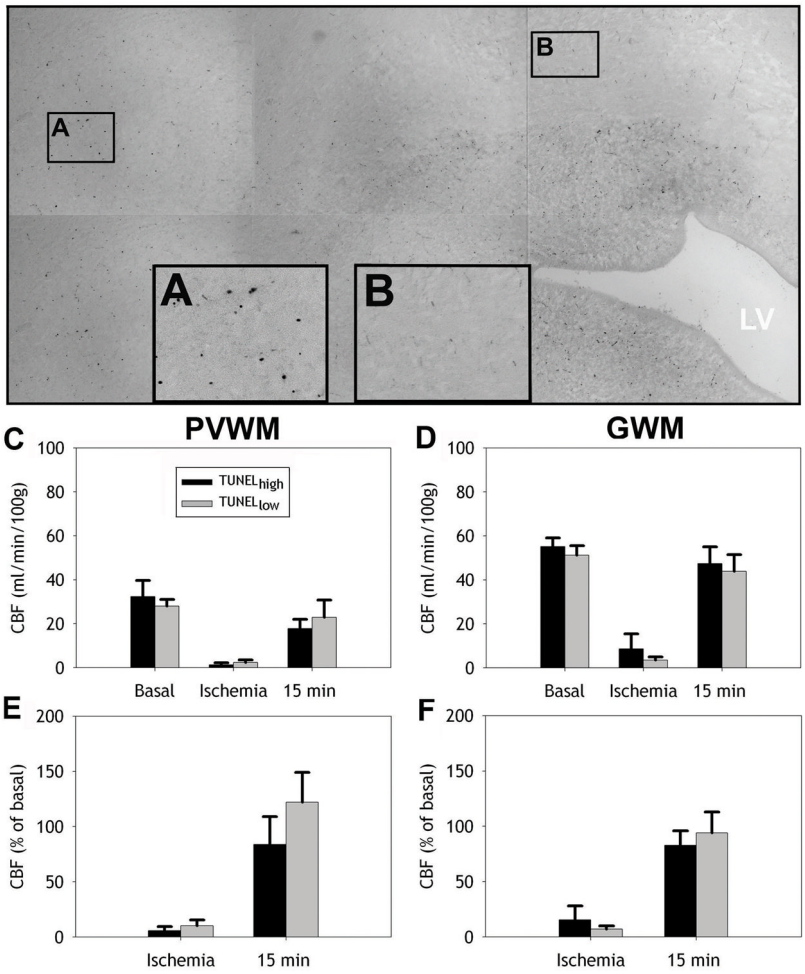

Figure 7.

Absolute and relative CBF in the PVWM and GWM are similar in regions of high and low injury defined by TUNEL staining. A, B, Representative high power images of $TUNEL_{high}$ (A) and $TUNEL_{low}$ (B) ROIs from a portion of a digitized montage in the PVWM. C, D, Absolute mean CBF (±SEM) during basal conditions, ischemia, and at 15 min reperfusion in regions classified as $TUNEL_{high}$ and $TUNEL_{low}$ for periventricular (PVWM; C) and gyral white matter (GWM; D). E, F, relative CBF during ischemia and at 15 min reperfusion in PVWM (E) and GWM (F).

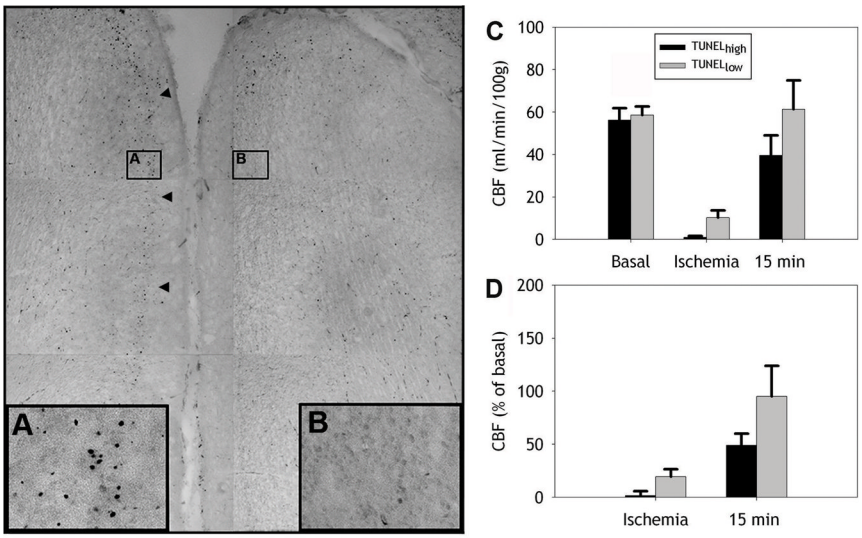

Figure 8.

The magnitude of cortical injury is predicted by the severity of ischemia. A, B, Representative high power images of $TUNEL_{high}$ (A) and $TUNEL_{low}$ (B) ROIs from a portion of a digitized montage of two adjacent frontal cortical gyri. C, Absolute mean CBF (±SEM) during basal conditions, ischemia, and at 15 min reperfusion in $TUNEL_{high}$ (black bars) and $TUNEL_{low}$ (gray bars) areas of cerebral cortex. During ischemia, areas with a higher density of TUNEL-labeled cells showed significantly less blood flow relative to $TUNEL_{low}$ areas (*p<0.005). D, Similarly relative CBF during ischemia and at 15 min reperfusion in these $TUNEL_{high}$ areas was also lower relative to $TUNEL_{low}$ areas but was not significant. Arrowheads point to cortical layers showing high TUNEL density.

Table 1

Absolute regional CBF values (mean ± SEM) and CBF values expressed as a percentage of basal CBF (bold represents significant deviation from 100%) during ischemia and reperfusion at 15 and 60 minutes, as obtained for 7 frontal and 4 parietal structures.

Frontal	**Ischemia (% basal CBF)**	**15 min (% basal CBF)**	**60 min (% basal CBF)**
Cortex	7 ± 2.2 (**11 ± 3.3**)	48± 10.2 (73 ± 15.1)	86 ± 4.8 **(132 ± 6.3)**
PVWM	7 ± 1.9 **(25 ± 7.8)**	26 ± 4.8 (97 ± 17.8)	34 ± 3.6 **(125 ±7.6)**
Corpus Callosum	3 ± 1.8 **(15 ± 8.6)**	26 ± 5.6 (151 ± 36.6)	38 ± 4.3 **(189 ± 29.8)**
Putamen	11 ± 2.9 **(14 ± 3.4)**	88 ± 9.1 (115 ± 14.3)	82 ± 11 (103± 8.9)
SVZ	7 ± 2.0 **(28 ± 9.3)**	29 ± 5.4 (101 ± 20.9)	37 ± 3.7 (128 ± 13.4)
Caudate Body	8 ± 2.4 **(11 ± 3.0)**	67 ± 7.4 (92 ± 10.9)	62 ± 4.6 (85 ± 7.0)
Caudate Head	8 ± 2.9 **(12 ± 4.1)**	61 ± 8.9 (101 ± 23.6)	69 ± 7.0 (115 ± 27.3)
Parietal	**Ischemia (% basal CBF)**	**15 min (% basal CBF)**	**60 min (% basal CBF)**
Cortex	6 ± 2.5 **(9 ± 3.5)**	49 ± 10.5 (74 ± 15.5)	87 ± 3.8 **(133 ± 8.6)**
PVWM	3 ± 1.0 **(14 ± 4.0)**	21 ± 3.8 (88 ± 16.7)	27 ± 2.2 (113 ± 12.1)
Hippocampus	7 ± 2.9 **(12 ±4.5)**	54 ± 5.9 (94 ± 12.1)	62 ± 3.5 (106 ± 8.8)
Thalamus	13 ± 4.1 **(13 ±3.9)**	117 ± 17.1 (123 ± 16.0)	109.5 ± 9.6 (118± 15.7)